Dynamic Modeling of Two Cooperating Flexible Manipulators

Jin-Soo Kim*
Commercial Vehicle Research Center, Hyundai Motor Company
Masaru Uchiyama
Department of Aeronautics and Space Engineering, Tohoku University

In this paper, our aim is to develop a model for two cooperating flexible manipulators handling a rigid object by using lumped parameters. This model is in turn analyzed on MATLAB. In order to validate the model, a precise simulation model is developed using ADAMS™(Automatic Dynamic Analysis of Mechanical System). Moreover, to clarify the discussion, the motions of a dual-arm experimental flexible manipulator are considered. Using the developed model, we control a robotic system with a symmetric hybrid position/force control scheme. Finally, experiments and simulations are performed, and a comparison of simulation results with experimental results is given to a rerify the validity of our model.

Key Words : Cooperative Control, Two Flexible Manipulator, Lumped-Parameter Model, Experimental Robot, ADAMS™, MATLAB

1. Introduction

In the past decade, a considerable amount of research effort has been devoted to single arm flexible manipulators, especially to their modeling, vibration control, inverse kinematics and inverse dynamics(Book et al., 1975; Judd and Falkenburg, 1985; Bayo, 1987; Ha and Park, 1993; Konno and Uchiyama, 1996). On the other hand, only a few publications discuss the application of flexible manipulators in contact tasks. Recently, some researchers have started studying the problem of position/force control, and some experiments have been conducted(Matsuno et al., 1994; Kim et al., 1997).

Furthermore, for applications beyond the capability of a single arm, for example the manipulation of bulky objects, coordination between multiple manipulators is necessary. However, publications on motion and force control of multiple cooperating flexible manipulators are shill few in number. An initial work may be found in Koike, Shimojima and Yamabe(Koike et al., 1996), in wich They propose a simple method for controlling the motion and grasping forces on a rigid object by two cooperating flexible manipulators without calculating the inverse dynamics. Sur and Murray have studied controllers developed for dual arm flexible robots in hybrid force/position control tasks, and have shown the effects of flexibility and its suitability for certain types of robotic tasks through experiments(Sur and Murray, 1997). Matsuno and Hatayama have addressed the dynamics of dual flexible manipulators by using the distributed-parameter model under quasi-static assumptions(Matsuno and Hatayama, 1996). In some multi-link flexible manipulators, the equations of motion depend upon the arm's configuration, and therefore real time computations are necessary. But these computations are quite difficult and time consuming if a distributed-parameter model is used. lumped-parameter models are more efficient for such purposes because of their simplicity.

Therefore, our aim is to develop a model for two cooperating flexible manipulators handling a rigid object by using lumped-parameters. Using

* Corresponding Author,
E-mail : j_s_kim@hyundai-motor.com
TEL : +82-652-260-6231 ; **FAX** : +81-652-260-6250
Commercial Vehicle Research Center, Hyundai Motor Company, 800 Yongam-ri, Bangdong, Wanju-gun, Chonbuk 565-900, Korea. (Manuscript **Received** May 10, 1999; **Revised** November 15, 1999)

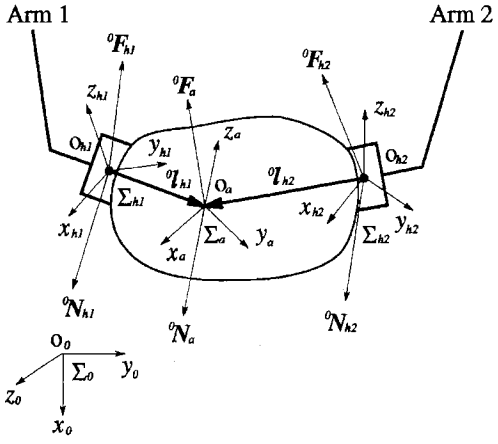

Fig. 1 Two arms holding an object

this model, we control robots with a symmetric hybrid position/force control scheme (Uchiyama and Dauchez, 1988).

2. Workspace Vectors for Coordination Task

Consider two robots holding a rigid object cooperatively as presented in Fig. 1. Let $\sum_0$, $\sum_{hi}$; $i=1, 2$, $\sum_a$ be the base reference frame, the frames of the end-effectors, and the frame fixed relative to the object, Let ${}^0\boldsymbol{F}_{h1}$, ${}^0\boldsymbol{F}_{h2}$ be the forces and ${}^0\boldsymbol{N}_{h1}$, ${}^0\boldsymbol{N}_{h2}$ be the moments exerted by hands 1 and 2 respectively. Consider the line between an end-effector and the object frame's center O_a as a rigid virtual stick (Uchiyama and Dauchez, 1988). To express the motion of the end-effector of the virtual stick, define the coordinate system $\sum_{bi}$ as shown in Fig. 2. If the deformation of the object and the slip between end-effector and the object is assumed to be small, $\sum_{ai}$ equals $\sum_{bi}$. The virtual sticks are represented by the vector $\boldsymbol{l}_{hi}$. Henceforth, we take $\boldsymbol{f}=[\boldsymbol{F}^T \ \boldsymbol{N}^T]^T$. The forces/moments ${}^0\boldsymbol{f}_{bi}$ at the tips of the virtual sticks O_{bi} can be easily calculated from ${}^0\boldsymbol{f}_{hi}$:

$$ {}^0\boldsymbol{f}_{bi}=\begin{bmatrix} \boldsymbol{I}_3 & 0 \\ \boldsymbol{L}_{hi} & \boldsymbol{I}_3 \end{bmatrix}^0 \boldsymbol{f}_{hi}={}^0\boldsymbol{D}_{hi}{}^0\boldsymbol{f}_{hi} \tag{1} $$

where $\boldsymbol{I}_3 \in \Re^{3\times 3}$ is the unit matrix and

$$ \boldsymbol{L}_{hi}=\begin{bmatrix} 0 & l_{hiz} & -l_{hiy} \\ -l_{hiz} & 0 & l_{hix} \\ l_{hiy} & -l_{hix} & 0 \end{bmatrix}. $$

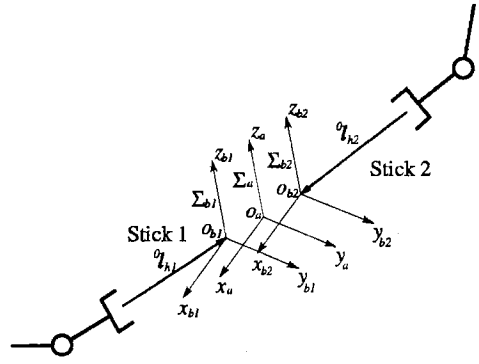

Fig. 2 Coordination with virtual stick

Applying the principle of virtual work done by the force of Eq. (1), the velocity relation can be obtained as

follows:

$$ {}^0\boldsymbol{s}_h={}^0\boldsymbol{D}_h^T \, {}^0\boldsymbol{s}_b \tag{2} $$

where ${}^0\boldsymbol{s}_{hi}=[{}^0\boldsymbol{v}_{hi}^T \ {}^0\boldsymbol{\omega}_{hi}^T]^T \in \Re^{6\times 1}$ is a vector denoting the Cartesian velocity at $\sum_{hi}$, ${}^0\boldsymbol{s}_{bi}=[{}^0\boldsymbol{v}_{bi}^T \ {}^0\boldsymbol{\omega}_{bi}^T]^T \in \Re^{6\times 1}$ is the vector denoting the Cartesian velocity at $\sum_{bi}$. The external forces/moments on the object due to each virtual stick can be presented in the following form:

$$ \begin{aligned} {}^0\boldsymbol{f}_a &=[\boldsymbol{I}_6 \ \boldsymbol{I}_6] \ [{}^0\boldsymbol{f}_{b1} \ {}^0\boldsymbol{f}_{b2}]^T \\ &=\boldsymbol{W}{}^0\boldsymbol{q}_b \end{aligned} \tag{3} $$

where $\boldsymbol{W} \in \Re^{6\times 12}$, which transforms the end-effector force to the object, possesses a nontrivial null space. This means that we can define an internal force/moment vector ${}^0\boldsymbol{f}_r$ by using the properties of the Moore-Penrose inverse such that

$$ {}^0\boldsymbol{q}_b=\boldsymbol{W}^+ \, {}^0\boldsymbol{f}_a+\boldsymbol{V} \, {}^0\boldsymbol{f}_r \tag{4} $$

where

$$ \boldsymbol{W}^+=\begin{bmatrix} \frac{1}{2}\boldsymbol{I}_6 & \frac{1}{2}\boldsymbol{I}_6 \end{bmatrix} $$

is the Moore-Penrose inverse of $\boldsymbol{W}$, and

$$ \boldsymbol{V}=[\boldsymbol{I}_6 \ -\boldsymbol{I}_6]^T. $$

Therefore, we can define the workspace force/moment vector ${}^0\boldsymbol{h}$ by combining the external force/moment vector ${}^0\boldsymbol{f}_a$ and internal force/moment vector ${}^0\boldsymbol{f}_r$ as follows:

$$ \begin{aligned} {}^0\boldsymbol{h} &=[{}^0\boldsymbol{f}_a^T \ {}^0\boldsymbol{f}_r^T]^T \\ &=\begin{bmatrix} ({}^0\boldsymbol{f}_{b1}+{}^0\boldsymbol{f}_{b2})^T & \frac{1}{2}({}^0\boldsymbol{f}_{b1}-{}^0\boldsymbol{f}_{b2})^T \end{bmatrix}^T. \end{aligned} \tag{5} $$

The position/orientation vector ${}^0\boldsymbol{z}$, containing the absolute position/orientation vector ${}^0\boldsymbol{p}_a$ of the object and the relative position/orientation vector ${}^0\boldsymbol{p}_r$ of the tips of virtual sticks can be defined as:

$$\begin{aligned}{}^0\boldsymbol{z}&=[{}^0\boldsymbol{p}_a^T\ {}^0\boldsymbol{p}_r^T]^T\\&=\left[\frac{1}{2}({}^0\boldsymbol{p}_{b1}+{}^0\boldsymbol{p}_{b2})^T\ \frac{1}{2}({}^0\boldsymbol{p}_{b1}-{}^0\boldsymbol{p}_{b2})^T\right]^T\end{aligned}\tag{6}$$

where $\boldsymbol{p}_{bi}$ represents the absolute position/orientation vector at the tip of stick i.

3. Dynamics of System

3.1 Manipulator models

In this section we develop the dynamic equations of two flexible manipulators holding a common rigid object. It is assumed that the end-effectors can furnish a tight grasp so that there is no relative motion between the end-effectors and the object. Thus a closed-loop kinematic chain mechanism is formed.

Using the lumped-parameter model (Konno and Uchiyorma, 1996), the dynamic model for the i-th manipulator, which is exerting a generalized contact force/moment ${}^0\boldsymbol{f}_{hi}$ on the object, is given by:

$$\begin{aligned}\begin{bmatrix}\boldsymbol{\tau}_i\\\boldsymbol{0}\end{bmatrix}&=\begin{bmatrix}\boldsymbol{M}_{i11}(\boldsymbol{q}_i)&\boldsymbol{M}_{i12}(\boldsymbol{q}_i)\\\boldsymbol{M}_{i21}(\boldsymbol{q}_i)&\boldsymbol{M}_{i22}(\boldsymbol{q}_i)\end{bmatrix}\begin{bmatrix}\ddot{\boldsymbol{\theta}}_i\\\ddot{\boldsymbol{e}}_i\end{bmatrix}\\&+\begin{bmatrix}\boldsymbol{h}_{i1}(\boldsymbol{q}_i,\ \dot{\boldsymbol{q}}_i)\\\boldsymbol{h}_{i2}(\boldsymbol{q}_i,\ \dot{\boldsymbol{q}}_i)\end{bmatrix}+\begin{bmatrix}0&0\\0&\boldsymbol{K}_{i22}\end{bmatrix}\begin{bmatrix}\boldsymbol{\theta}_i\\\boldsymbol{e}_i\end{bmatrix}\\&+\begin{bmatrix}\boldsymbol{g}_{i1}(\boldsymbol{q}_i)\\\boldsymbol{g}_{i2}(\boldsymbol{q}_i)\end{bmatrix}+\begin{bmatrix}\boldsymbol{j}_{hi\theta}^T(\boldsymbol{q}_i)\\\boldsymbol{j}_{hie}^T(\boldsymbol{q}_i)\end{bmatrix}{}^0\boldsymbol{f}_{hi}\end{aligned}\tag{7}$$

or in compact form

$$\begin{aligned}\boldsymbol{L}\boldsymbol{\tau}_i=&\boldsymbol{M}_i(\boldsymbol{q}_i)\ \ddot{\boldsymbol{q}}_i+\boldsymbol{h}_i(\boldsymbol{q}_i,\ \dot{\boldsymbol{q}}_i)+\boldsymbol{K}_i\boldsymbol{q}_i\\&+\boldsymbol{g}_i(\boldsymbol{q}_i)+\boldsymbol{j}_{hi}^T(\boldsymbol{q}_i)\,{}^0\boldsymbol{f}_{hi}\end{aligned}\tag{8}$$

where $\boldsymbol{q}_i=[\boldsymbol{\theta}_i^T\ \boldsymbol{e}_i^T]$ are the generalized coordinates, $\boldsymbol{\theta}_i\in\Re^n$ is a vector of the joint angles and $\boldsymbol{e}_i\in\Re^m$ is a vector of the elastic deflections, and $\boldsymbol{M}_{i11}\in\Re^{n\times n}$, $\boldsymbol{M}_{i12}\in\Re^{n\times m}$, $\boldsymbol{M}_{i21}\in\Re^{m\times n}$ and $\boldsymbol{M}_{i22}\in\Re^{m\times m}$ are submatrices of the inertia matrix. $\boldsymbol{h}_{i1}$ and $\boldsymbol{h}_{i2}$ are vectors of the centrifugal and the Coriolis forces, $\boldsymbol{g}_{i1}$ and $\boldsymbol{g}_{i2}$ are gravity vectors, $\boldsymbol{K}_{i22}\in\Re^{m\times m}$ is the stiffness matrix, $\boldsymbol{J}_{hi\theta}\in\Re^{6\times n}$ and $\boldsymbol{J}_{hie}\in\Re^{6\times m}$ are constraint Jacobian matrices, and $\boldsymbol{\tau}_i\in\Re^n$ is the joint torque vector.

From Eqs. (1) and (2), the Jacobian can be computed as:

$$\boldsymbol{J}_{hi}={}^0\boldsymbol{D}_{hi}^T\boldsymbol{J}_{bi}.\tag{9}$$

From Eqs. (1) and (9), we can obtain:

$$\boldsymbol{J}_{hi}^T(\boldsymbol{q}_i)\,{}^0\boldsymbol{f}_{hi}=\boldsymbol{J}_{bi}^T(\boldsymbol{q}_i)\,{}^0\boldsymbol{f}_{bi}.\tag{10}$$

We can rewrite the above dynamics equations as:

$$\begin{aligned}\boldsymbol{L}\boldsymbol{\tau}_i=&\boldsymbol{M}_i(\boldsymbol{q}_i)\ \ddot{\boldsymbol{q}}_i+\boldsymbol{h}_i(\boldsymbol{q}_i,\ \dot{\boldsymbol{q}}_i)+\boldsymbol{K}_i\boldsymbol{q}_i\\&+\boldsymbol{g}_i(\boldsymbol{q}_i)+\boldsymbol{j}_{bi}^T(\boldsymbol{q}_i)\,{}^0\boldsymbol{f}_{bi}.\end{aligned}\tag{11}$$

3.2 Object dynamics

The dynamics model of the object can be obtained using the Newton-Euler equation. Expressed in the object fixed frame O_a, these equations can be written as follows:

$$\begin{aligned}{}^0\boldsymbol{f}_a&={}^0\boldsymbol{f}_{b1}+{}^0\boldsymbol{f}_{b2}\\&=\begin{bmatrix}m_a\boldsymbol{I}_3&\boldsymbol{0}\\\boldsymbol{0}&\boldsymbol{I}_a\end{bmatrix}\begin{bmatrix}{}^0\dot{\boldsymbol{v}}_a\\{}^0\dot{\boldsymbol{\omega}}_a\end{bmatrix}\\&+\begin{bmatrix}\boldsymbol{0}\\{}^0\boldsymbol{\omega}_a\times\boldsymbol{I}_a{}^0\boldsymbol{\omega}_a\end{bmatrix}+\begin{bmatrix}m_a\boldsymbol{g}\\\boldsymbol{0}\end{bmatrix}\end{aligned}\tag{12}$$

or in more compact form as

$${}^0\boldsymbol{f}_a=\boldsymbol{\Psi}_a{}^0\dot{\boldsymbol{s}}_a+\boldsymbol{h}_a(\boldsymbol{s}_a)+\boldsymbol{g}_a\tag{13}$$

where $\boldsymbol{I}_a\in\Re^{3\times3}$ is the inertial matrix of the object about O_a, ${}^0\boldsymbol{\omega}_a=[{}^0\boldsymbol{\omega}_{ax}\ {}^0\boldsymbol{\omega}_{ay}\ {}^0\boldsymbol{\omega}_{az}]$, $\boldsymbol{h}_a$ is the vector of the centrifugal and the Coriolis forces, $\boldsymbol{g}_a$ is the gravity vector, and ${}^0\boldsymbol{s}_a=[{}^0\boldsymbol{v}_a\ {}^0\boldsymbol{\omega}_a]$ is the velocity vector. Eq. (13) can be transformed into joint space as:

$$\begin{aligned}\boldsymbol{f}_a&=\boldsymbol{\Psi}_a\boldsymbol{J}_{bi}(\boldsymbol{q}_i)\ \ddot{\boldsymbol{q}}_i+\boldsymbol{\Psi}_a\dot{\boldsymbol{J}}_{bi}(\dot{\boldsymbol{q}}_i)\,\boldsymbol{q}_i+\boldsymbol{h}_a(\boldsymbol{s}_a)+\boldsymbol{g}_a\\&=\boldsymbol{\Psi}_a\boldsymbol{J}_{bi}(\boldsymbol{q}_i)\ \ddot{\boldsymbol{q}}_i+\hat{\boldsymbol{h}}_a(\boldsymbol{q}_1,\ \dot{\boldsymbol{q}}_1)+\boldsymbol{g}_a.\end{aligned}\tag{14}$$

3.3 Kinematic coupling

The system is kinematically coupled because both the manipulators and object form a closed chain. Expressing the Cartesian velocity of the mass center of the object, we have the following relationship:

$$[{}^0\boldsymbol{v}_a^T\ {}^0\boldsymbol{\omega}_a^T]^T=[{}^0\boldsymbol{v}_{bi}^T\ {}^0\boldsymbol{\omega}_{bi}^T]^T=\boldsymbol{J}_{bi}(\boldsymbol{q}_i)\ \dot{\boldsymbol{q}}_i.\tag{15}$$

From the above equation, the equations obtained for $i=1,\ 2$ are:

$$[\hat{\boldsymbol{J}}_{b\theta}\ \ \hat{\boldsymbol{J}}_{be}]\begin{bmatrix}\boldsymbol{\theta}\\\boldsymbol{e}\end{bmatrix}=\boldsymbol{0}_{6\times1}\tag{16}$$

where

$$\hat{J}_{b\theta}=[J_{b\theta 1} \quad -J_{b\theta 2}]$$
$$\hat{J}_{be}=[J_{be1} \quad -J_{be2}]$$

The constraint matrix A is defined as:

$$A(q)=[\hat{J}_{b\theta} \quad \hat{J}_{be}]. \tag{17}$$

Therefore, the kinematic constraint equation becomes:

$$A(q)\dot{q}=0_{6\times 1} \tag{18}$$

where $A(q)\in\Re^{6\times 2(n+m)}$ is assumed to have rank six. The corresponding acceleration constraints result by differentiating Eq. (18):

$$A(q)\ddot{q}+\dot{A}(q)\dot{q}=0_{6\times 1}. \tag{19}$$

4. Closed Chain Model in Joint Space

Substituting Eqs. (4), (13) and (15) into Eq. (11), the dynamics of the closed chain system consisting of two manipulators and an object is obtained as:

$$\begin{bmatrix}\tau\\0\end{bmatrix}=\begin{bmatrix}M_{11}(q) & M_{12}(q)\\ M_{21}(q) & M_{22}(q)\end{bmatrix}\begin{bmatrix}\ddot{\theta}\\ \ddot{e}\end{bmatrix}+\begin{bmatrix}h_1(q,\dot{q})\\ h_2(q,\dot{q})\end{bmatrix}+\begin{bmatrix}0 & 0\\ 0 & K_{22}\end{bmatrix}\begin{bmatrix}\theta\\ e\end{bmatrix}+\begin{bmatrix}g_1(q)\\ g_2(q)\end{bmatrix}+\begin{bmatrix}\hat{J}^T_{b\theta}(q)\\ \hat{J}^T_{be}(q)\end{bmatrix}{}^0f_r \tag{20}$$

where

$$\tau=[\tau_1^T \quad \tau_2^T]^T \quad \theta=[\theta_1^T \quad \theta_2^T]^T$$
$$e=[e_1^T \quad e_2^T]^T \quad K_{22}=\mathrm{diag}[K_{i22}]$$
$$M_s=\mathrm{diag}[M_{is}+\frac{1}{2}\hat{J}^T_{bi\theta}\Psi_a\hat{J}_{bi\theta}]$$
$$h_1=[h_{11}+\frac{1}{2}\hat{J}^T_{b1\theta}h_a \quad h_{21}+\frac{1}{2}\hat{J}^T_{b2\theta}h_a]^T$$
$$h_2=[h_{12}+\frac{1}{2}\hat{J}^T_{b1e}h_a \quad h_{22}+\frac{1}{2}\hat{J}^T_{b2e}h_a]^T$$
$$g_1=[g_{11}+\frac{1}{2}\hat{J}^T_{b1\theta}g_a \quad g_{21}+\frac{1}{2}\hat{J}^T_{b2\theta}g_a]^T$$
$$g_2=[g_{12}+\frac{1}{2}\hat{J}^T_{b1e}g_a \quad g_{22}+\frac{1}{2}\hat{J}^T_{b2e}g_a]^T$$

$s=11$, 12, 21, and 22. Equation (20) can be rewritten in the following more compact form:

$$L\tau=M(q)\ddot{q}+h(q,\dot{q})+Kq+g(q)+A^T\,{}^0f_r. \tag{21}$$

Equation (21) can be solved for the generalized acceleration vector $\ddot{q}$, which is then substituted into Eq. (19) to yield

$$AM^{-1}A^T\,{}^0f_r=\dot{A}(q)\dot{q}+AM^{-1}\{L\tau-h-Kq-g\}. \tag{22}$$

Since A has rank six, the matrix on the left-hand side of Eq. (22) is nonsingular and this equation can be solved for ${}^0f_r$. The closed chain dynamics is determined by eliminating the vector ${}^0f_r$ in Eq. (21) using Eq. (22). After rearranging, the resulting equation becomes:

$$\eta\{L\tau-h-Kq-g\}=M\ddot{q}+A^T(AM^{-1}A^T)^{-1}\dot{A}\dot{q} \tag{23}$$

where $\eta(q)\in\Re^{2(n+m)\times 2(n+m)}$ is defined as:

$$\eta=I_{2(n+m)}-A^T(AM^{-1}A^T)^{-1}AM^{-1}.$$

5. Experimental Setup

5.1 A manipulator system

The experimental manipulator named "ADAM" (Aerospace Dual Arm Manipulator) has two arms (Fig. 3), each of which consists of 2 elastic links and 7 rotary joints (Uchiyama et al., 1990). The parameters of each link are

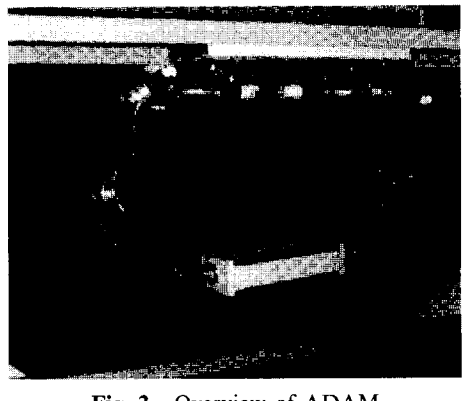

Fig. 3 Overview of ADAM

Table 1 ADAM link parameters

	Link 3	Link 5
Length	0.5 [m]	0.5 [m]
Elastic part	0.359 [m]	0.394 [m]
Diameter	0.013 [m]	0.01 [m]
Material	SUP-6	SUP-6
EI	288.1 [Nm^2]	100.8 [Nm^2]
GJ	224.32 [Nm^2[	78.54 [Nm^2]
Mass	0.7 [kg]	0.5 [kg]

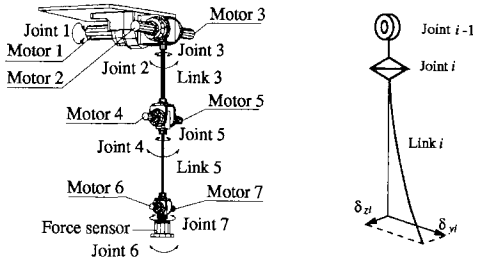

Fig. 4 Joints, motors, links and link deflections of Arm2(i=3, 5)

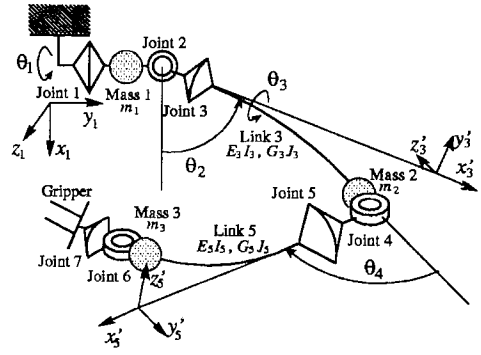

Fig. 5 Lumped-parameter model of the experimental manipulator ADAM

presented in Table 1. Both arms in the cooperative manipulation system have the same parameters. In this paper, the discussion is restricted to motions of joints 2, 4 and 6 only.

5.2 Modeling of ADAM

Figure 5 shows the lumped-masses (*stations*) and massless springs model for the left arm only. The lumped masses are considered as concentrated at the tips of the respective links while the links themselves are considered as massless springs with elastic and torsional properties as E_3I_3, E_5I_5 and G_3J_3, G_5J_5, respectively. The joint angle vector $\boldsymbol{\theta}$ and the link deflection vector $\boldsymbol{e}$ are respectively:

$$\boldsymbol{\theta}=[\theta_{12}\ \theta_{14}\ \theta_{16}\ \theta_{22}\ \theta_{24}\ \theta_{26}]^T$$
$$\boldsymbol{e}=[\delta_{y13}\ \delta_{z13}\ \delta_{y15}\ \delta_{z15}\ \delta_{y23}\ \delta_{z23}\ \delta_{y25}\ \delta_{z25}]^T$$

where δ_{yi3}, δ_{yi5}, δ_{zi3} and δ_{zi5} are elastic deflections along the y and z axes of links 3 and 5 for the i-th manipulator, respectively.

5.3 Hybrid position/force Control

For a manipulator equipped with velocity feedback servo motors, the relationship between the velocity commands and the produced torques can be written as

$$\begin{aligned}\boldsymbol{\tau}&=\boldsymbol{G}_r\boldsymbol{K}_{sp}(\boldsymbol{V}_{ref}-\boldsymbol{K}_{sv}\dot{\boldsymbol{\theta}}_m)\\&=\boldsymbol{\Lambda}(\dot{\boldsymbol{\theta}}_c-\dot{\boldsymbol{\theta}})\end{aligned}\tag{24}$$

where $\dot{\boldsymbol{\theta}}_m(=\boldsymbol{G}_r\dot{\boldsymbol{\theta}})$ is the angular velocity vector of the motors, $\boldsymbol{V}_{ref}$[V] is the voltage/velocity command vector for the manipulator, $\boldsymbol{K}_{sp}$ [Nm/V], $\boldsymbol{K}_{sv}$ [Vs/rad] and $\boldsymbol{G}_r$ are diagonal matrices whose diagonal elements are the velocity servo gains, the voltage/velocity coefficients and the gear reduction ratios, respectively. $\dot{\boldsymbol{\theta}}_c$ is the velocity command vector, and $\boldsymbol{\Lambda}(=\boldsymbol{G}_r^2\boldsymbol{K}_{sp}\boldsymbol{K}_{sv})$ gives the velocity feedback gains. The voltage velocity command vector $\boldsymbol{V}_{ref}$ is computed by:

$$\boldsymbol{V}_{ref}=\boldsymbol{G}_r\boldsymbol{K}_{sv}\dot{\boldsymbol{\theta}}_c\tag{25}$$

and is used in the experiments.

In this paper, we have utilized the symmetric hybrid control principle proposed by M. Uchiyama and P. Dauchez (1988). The task vectors for the hybrid position/force control are defined as

$$\begin{aligned}\boldsymbol{h}&=\boldsymbol{H}\ {}^0\boldsymbol{h}=[{}^0\boldsymbol{f}_a^T\ {}^a\boldsymbol{f}_r^T]^T\\\boldsymbol{z}&=\boldsymbol{H}\boldsymbol{B}_r{}^0\boldsymbol{z}=[{}^0\boldsymbol{p}_a^T\ {}^a\boldsymbol{p}_r^T]^T\end{aligned}\tag{26}$$

where $\boldsymbol{H}=\mathrm{diag}[\boldsymbol{I}_6\ {}^a\boldsymbol{R}_0]$, $\boldsymbol{B}_r=\mathrm{diag}[\boldsymbol{I}_6\ \boldsymbol{B}_s]$, the external workspace vector $({}^0\boldsymbol{f}_a, {}^0\boldsymbol{p}_a)$ and internal workspace vector $({}^a\boldsymbol{f}_r, {}^a\boldsymbol{p}_r)$ are represented with respect to $\sum_0$ and $\sum_a$ respectively. ${}^a\boldsymbol{R}_0\in\Re^{6\times6}$ is a rotational matrix from $\sum_0$ to $\sum_a$ and $\boldsymbol{B}_s\in\Re^{6\times6}$ is a matrix that transforms the time derivative of the orientation vector of a frame into its rotational velocity.

The joint velocity command vector $\dot{\boldsymbol{\theta}}_c$ is computed as:

$$\dot{\boldsymbol{\theta}}_c=\dot{\boldsymbol{\theta}}_z+\dot{\boldsymbol{\theta}}_h\tag{27}$$

where $\dot{\boldsymbol{\theta}}_z$ is the joint velocity vector for positioning and is calculated by

$$\dot{\boldsymbol{\theta}}_z=\boldsymbol{J}_{D\theta}^{-1}\boldsymbol{S}\boldsymbol{K}_{zp}\boldsymbol{B}_a(\boldsymbol{z}_d-\boldsymbol{z})\tag{28}$$

and $\dot{\boldsymbol{\theta}}_h$ is the joint velocity vector for force control, and is calculated as

$$\dot{\boldsymbol{\theta}}_h=\boldsymbol{\Lambda}^{-1}\boldsymbol{J}_{D\theta}^T(\boldsymbol{I}_{12}-\boldsymbol{S})\boldsymbol{K}_{hp}(\boldsymbol{h}_d-\boldsymbol{h}).\tag{29}$$

$\boldsymbol{B}_a$ in Eq. (28) is a matrix that transforms the errors of orientation angles into a rotation vector. $\boldsymbol{S}$ and $(\boldsymbol{I}-\boldsymbol{S})$ define the matrices which respectively select position and force control directions. $\boldsymbol{K}_{zp}$ is a proportional gain matrix for positioning while $\boldsymbol{K}_{hp}$ is one for force control. In the hybrid position/force control with a virtual stick, using the velocity relationships between joint space and operational space, the Jacobian matrix $\boldsymbol{J}_{D\theta}$ is computed as

$$\boldsymbol{J}_{D\theta}=\boldsymbol{H}\boldsymbol{U}^T\boldsymbol{J}_{Db\theta}, \tag{30}$$

where $\boldsymbol{J}_{Db\theta}=\mathrm{diag}[\boldsymbol{J}_{bi\theta}]$.

5.4 Simulation model

Substituting Eq. (24) into Eq. (23) and taking into account the fact that $\dot{\boldsymbol{\theta}}=\boldsymbol{L}^T\dot{\boldsymbol{q}}$, the equations of motion of the coordinating flexible manipulator system are obtained as:

$$\boldsymbol{M}\ddot{\boldsymbol{q}}=-\boldsymbol{D}\dot{\boldsymbol{q}}+\eta\boldsymbol{L}\boldsymbol{\Lambda}\dot{\boldsymbol{\theta}}_c-\eta\boldsymbol{K}\boldsymbol{q}-\eta(\boldsymbol{h}+\boldsymbol{g}) \tag{31}$$

where

$$\boldsymbol{D}=\eta\boldsymbol{L}\boldsymbol{\Lambda}\boldsymbol{L}^T+\boldsymbol{A}^T(\boldsymbol{A}\boldsymbol{M}^{-1}\boldsymbol{A}^T)^{-1}\dot{\boldsymbol{A}}.$$

Equation (31) can be transformed into state space form as:

$$\begin{bmatrix}\ddot{\boldsymbol{q}}\\ \dot{\boldsymbol{q}}\end{bmatrix}=\begin{bmatrix}-\boldsymbol{D} & -\boldsymbol{M}^{-1}\eta\boldsymbol{K}\\ \boldsymbol{I} & \boldsymbol{0}\end{bmatrix}\begin{bmatrix}\dot{\boldsymbol{q}}\\ \boldsymbol{q}\end{bmatrix}+\begin{bmatrix}\boldsymbol{M}^{-1}\eta\boldsymbol{L}\boldsymbol{\Lambda}\\ -\boldsymbol{M}^{-1}\eta\end{bmatrix}[\dot{\boldsymbol{\theta}}_c\ (\boldsymbol{g}+\boldsymbol{h})]. \tag{32}$$

Equation (32) can be cast into state space form as follows:

$$\dot{\boldsymbol{x}}=\boldsymbol{A}\boldsymbol{x}+\boldsymbol{B}\dot{\boldsymbol{\theta}}_{sc} \tag{33}$$

where $\dot{\boldsymbol{\theta}}_{sc}=[\dot{\boldsymbol{\theta}}_c\ (\boldsymbol{g}+\boldsymbol{h})]$. In simulations, the discrete-time state equation corresponding to Eq. (33) is used in the following form:

$$\boldsymbol{x}(k+1)=\boldsymbol{\Phi}\boldsymbol{x}(k)+\boldsymbol{\Gamma}\dot{\boldsymbol{\theta}}_{sc}(k), \tag{34}$$

where k indicates the k-th interval of the sampling process, and $\boldsymbol{\Phi}$ and $\boldsymbol{\Gamma}$ are the discrete versions of matrices $\boldsymbol{A}$ and $\boldsymbol{B}$ for a zero-order holder (ZOH).

5.5 A precise simulation model

A precise model of the ADAM robot is constructed by ADAMS™. In this simulator, a finite-element method based on Timosenko beam theory is used as a modeling technique for flexible structures. We consider our experimental manipulator as having 5 beam elements. A simple model of Coulomb friction is included in order to obtain a realistic simulation model reflecting experimental conditions. When the end-effector velocities become -0.001 [m/s] and 0.001 [m/s], the friction forces become $-\mu f_n$ [N] and μf_n [N], respectively, where μ is the friction constant. This friction model is recommended to be used with ADAMS™.

6. Experiments and Simulations

We present experimental and simulations results for the case when the end-effector is moving only in the y direction while applying a desired internal force of 10 [N] and a desired moment of 0.5 [Nm]. The responses of task motion and force/moment at the tip as achieved from simulations and experiments are shown in Fig. 7 and Fig. 8. We set $\boldsymbol{K}_{zp}=4.0\boldsymbol{I}_6[\mathrm{s}^{-1}]$ and $\boldsymbol{K}_{hp}=0.4\boldsymbol{I}_6$.

The sampling time is set as 15 [ms], and for these simulations K_{sp} of Eq. (24) is set to approximate the experimental results. The environmental stiffness and the friction constants are taken as 10000 [N/m] and 0.2, respectively, in the simulation model. In Fig. 8, "Adams" stands for results obtained from the ADAMS simulation software, while "Matlab" stands for the results obtained

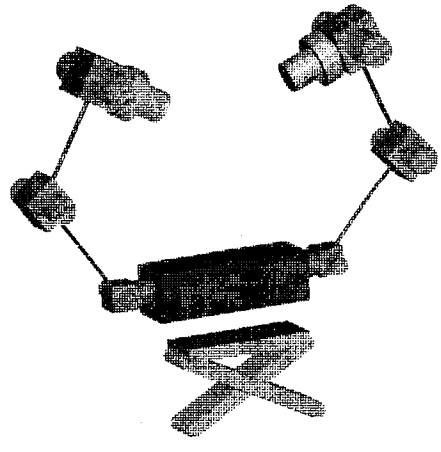

Fig. 6 ADAMS™ simulation model

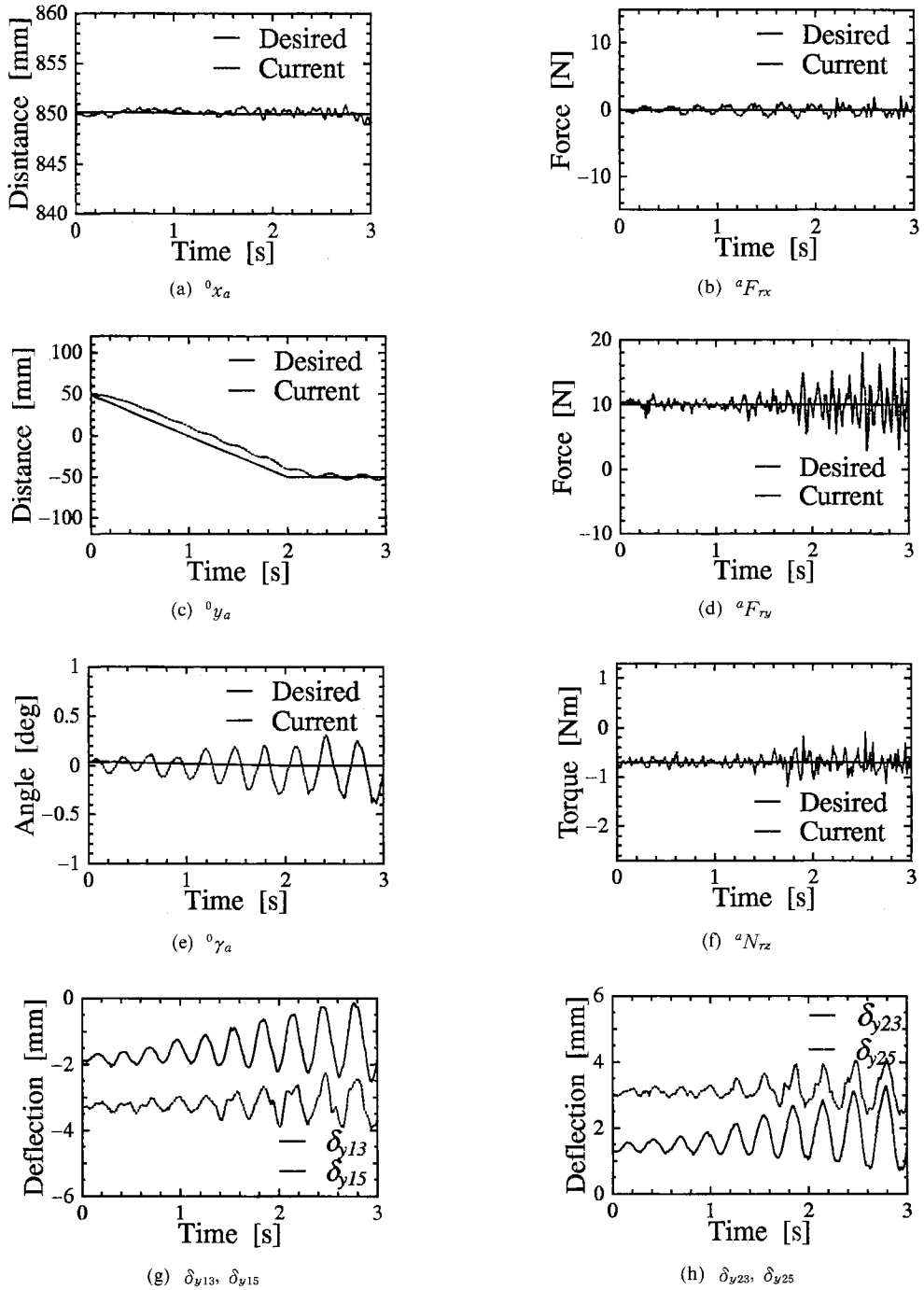

Fig. 7 Experimental results

from the MATLAB simulation. The reason for the system unstability of Fig. 6 (e) ~ (h), Fig. 7 (e) ~ (j) is the result of ignoring the effect of slip between the end-effectors of the manipulators and the object. Also, it shows the trend of vibration of one end-effector being transferred to the other end-effector through the object.

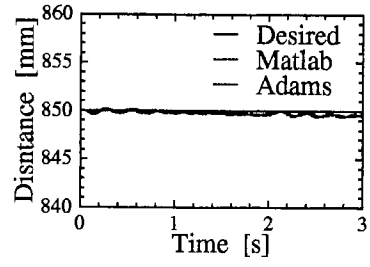

(a) ${}^{0}x_a$

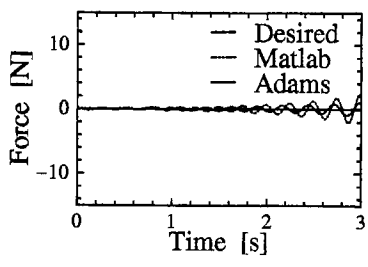

(b) ${}^{a}F_{rx}$

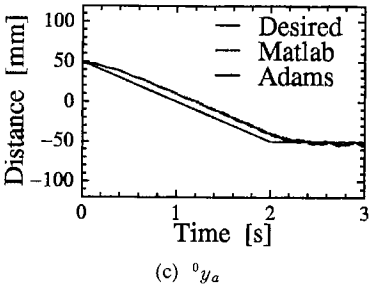

(c) ${}^{0}y_a$

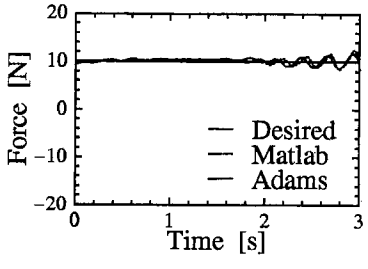

(d) ${}^{a}F_{ry}$

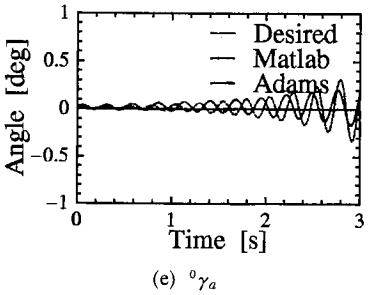

(e) ${}^{0}\gamma_a$

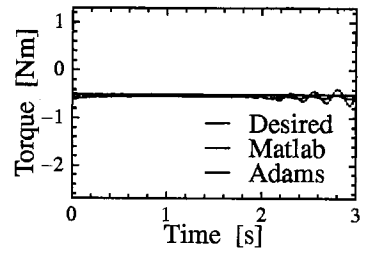

(f) ${}^{a}N_{rz}$

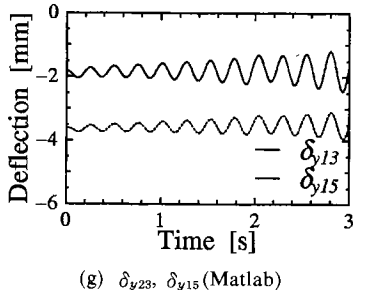

(g) δ_{y23}, δ_{y15}(Matlab)

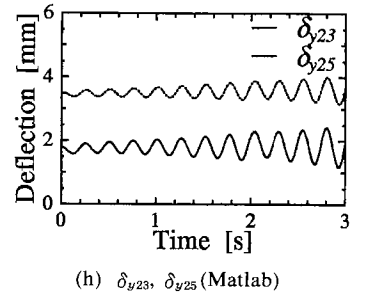

(h) δ_{y23}, δ_{y25}(Matlab)

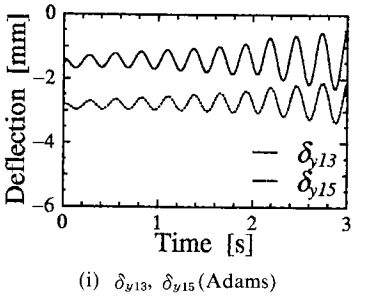

(i) δ_{y13}, δ_{y15}(Adams)

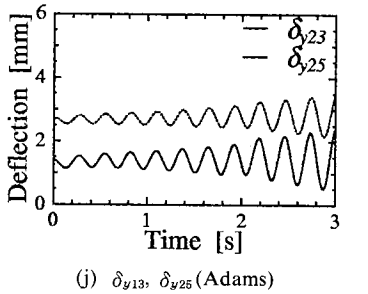

(j) δ_{y13}, δ_{y25}(Adams)

Fig. 8 Simulation results

7. Conclusions

This paper has developed a model for two cooperating flexible manipulators handling a rigid object by using lumped-parameters. A symmetric hybrid position/force control scheme for cooperating flexible manipulators has been presented. The control scheme has been further studied for an experimental flexible manipulator system. In order to valid at the lumped mass parameter modeling method for cooperating control of multi-manipulators, the MATLAB results of the model using the lumped mass parameter method, the ADAMS results of the model using distributed parameter modeling, and the experimental results were compared. Experimental results show that the system responses are in good agreement with simulation results. From these results, it was verified that the lumped mass parameter is valid for the cooperating control of multi-manipulators.

References

Bayo, E., 1987, "A Finite-Element Approach to Control the End-Point Motion of a Single-Link Flexible Robot," *J. Robotic Systems*, Vol. 4, No. 1, pp. 63~75.

Book, W. J. Neto, O. M. and Whitney, D. E., 1975, "Feedback Control of Two Beam, Two Joint Systems With Distributed Flexibility," *Trans. ASME, J. Dynam. Sys. Measurement and Control*, Vol. 97, pp. 424~431.

Ha, Y. K. and Park, Y. P., 1993, "Active Control of Flexible 3 DOF Robot Arm Vibration (I)," *A Journal of KSME*, Vol. 17, No. 3, pp. 548~558.

Judd, R. P. and Falkenburg, D. R., 1985, "Dynamics of Nonrigid Articulated Robot Linkages," *IEEE Trans. Automatic Control*, Vol. 30, No. 5, pp. 499~502.

Kim, J. S., Suzuki, K., Yamano, M. and Uchiyama, M., 1997, "Vibration Suppression Control of Constrained Spatial Flexible Manipulators," *Proc. of the IEEE Int. Conf. on Robotics and Automation*, Vol. 4, pp. 2831~2837.

Koike, S., Shimojima, H. and Yamabe, K., 1996, "Motion and Force Controls of Dual Flexible Manipulators with Velocity-Controlled DC Motors," *Trans. Japan Society of Mechanical Engineers*, Vol. 32, No. 4, pp. 547~556. (in Japanese).

Konno, A. and Uchiyama, M., 1996, "Modeling of a Flexible Manipulator Dynamics Based Upon Holzer's Model," *Proc. IEEE/RSJ Int. Conf. Intelligent Robots and Systems*, Vol. 1, pp. 223~229.

Matsuno, F. and Hatayama, M., 1996, "Quasi-Static Cooperative Control of Two-Link Flexible Manipulator," *Trans. Society of Instrument and Control Engineers*, Vol. 32, No. 4, pp. 547~556. (In Japanese).

Matsuno, F., Asano, T. and Sakawa, Y., 1994, "Modeling and Quasi-Static Hybrid Position/Force Control of a Constrained Planar Two-Link Flexible Manipulator," *IEEE Trans. on Robotics and Automation*, Vol. 10, No. 3, pp. 287~297.

Sur, S. and Murray, R. M., 1997, "An Experimental Comparison of Tradeoffs in Using Compliant Manipulators for Robotic Grasping Tasks," *Proc. of the IEEE Int. Conf. on Robotics and Automation*, Vol. 1, pp. 1807~1814.

Uchiyama, M. and Dauchez, P., 1988, "Symmetric Hybrid Position/Force Control Scheme for the Coordination of Two Robot," *Proc. of the IEEE Int. Conf. on Robotics and Automation*, Vol. 1, pp. 86~92.

Uchiyama, M., Konno, A., Uchiyama, T. and Kanda, S., 1990, "Development of a Flexible Dual-Arm Manipulator Testbed for Space Robotics," *Proc. of the IEEE Int. Workshop on Intelligent Robotics and Systems*, pp. 375~381.